

Computation of Nonretarded London Dispersion Coefficients and Hamaker Constants of Copper Phthalocyanine

Yan Zhao,* Hou T. Ng, and Eric Hanson

*Commercial Print Engine Lab, HP Laboratories, Hewlett-Packard Co.,
1501 Page Mill Road, Palo Alto, California 94304*

Jiannan Dong, David S. Corti, and Elias I. Franses

*School of Chemical Engineering, Purdue University, 480 Stadium Mall Drive,
West Lafayette, Indiana 47907-2100*

Received August 14, 2009

Abstract: A time-dependent density functional theory (TDDFT) scheme has been validated for predictions of the dispersion coefficients of five molecules (H_2O , NH_3 , CO_2 , C_6H_6 , and pentane) and for predictions of the static dipole polarizabilities of three organometallic compounds (TiCl_4 , OsO_4 , and $\text{Ge}(\text{CH}_3)_4$). The convergence of grid spacing has been examined, and two types of pseudopotentials and 13 density functionals have been tested. The nonretarded Hamaker constants A_{11} are calculated by employing a semiempirical parameter a along with the standard Hamaker constant equation. The parameter a is optimized against six accurate Hamaker constants obtained from the full Lifshitz theory. The dispersion coefficients of copper phthalocyanine CuPc and CuPc– SO_3H are then computed. Using the theoretical densities of $\rho_1 = 1.63$ and 1.62 g/cm^3 , the Hamaker constants A_{11} of crystalline α -CuPc and β -CuPc are found to be 14.73×10^{-20} and $14.66 \times 10^{-20} \text{ J}$, respectively. Using the experimentally derived density of $\rho_1 = 1.56 \text{ g/cm}^3$ for a commercially available β -CuPc (nanoparticles of $\sim 90 \text{ nm}$ hydrodynamic diameter), $A_{11} = 13.52 \times 10^{-20} \text{ J}$ is found. Its corresponding effective Hamaker constant in water (A_{121}) is calculated to be $3.07 \times 10^{-20} \text{ J}$. All computed A_{11} values for CuPc are noted to be higher than those reported previously.

1. Introduction

van der Waals interactions play key roles in numerous physical phenomena and applications, such as in crystal packing, colloidal stability, interfacial adhesion, self-assembly, molecular recognition, protein folding, nucleobases stacking, drug intercalation, solvation, supramolecular chemistry, pigment dispersion, and capillarity of liquids. The London dispersion forces are the major component of the long-range interparticle forces between nanoparticles or between colloidal particles. Those forces are described to first order by the macroscopic Hamaker constant.¹ This material-dependent quantity is difficult to measure experimen-

tally.^{2,3} Although the Hamaker constant can be calculated from Lifshitz's continuum theory,⁴ it requires detailed molecular and macroscopic information on the dielectric or optical properties of the material over a wide frequency range. These methods can pose a challenge for estimating Hamaker constants for many materials. Simplified models based on more recent extensions of the Lifshitz theory have been proposed.^{5–10}

In this Article, a computational approach based on time-dependent density functional theory (TDDFT) is benchmarked for predictions of the London dispersion coefficients (C_{11}) of five molecules (H_2O , NH_3 , CO_2 , C_6H_6 , and pentane) and for predictions of the static dipole polarizabilities of three organometallic compounds (TiCl_4 , OsO_4 , and $\text{Ge}(\text{CH}_3)_4$). The

* Corresponding author e-mail: yan.zhao3@hp.com.

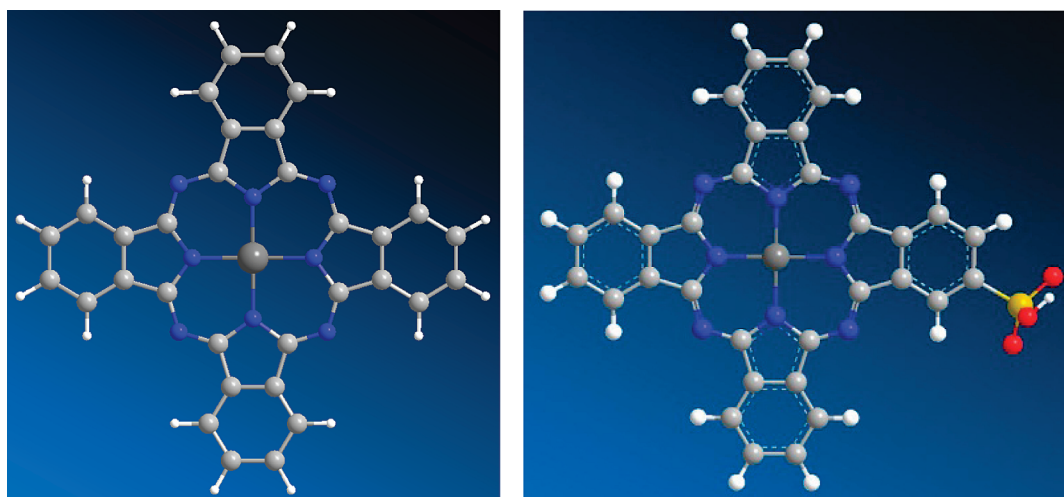


Figure 1. Molecular structures of CuPc ($C_{32}H_{16}CuN_8$, mol wt = 576.1) and CuPc- SO_3H ($C_{32}H_{16}CuN_8\text{SO}_3$, mol wt = 656.1).

validated TDDFT scheme is then employed to calculate the dispersion coefficients for copper phthalocyanine (CuPc), and for monosulphonated CuPc (CuPc- SO_3H), which are important for certain ink pigments. The molecular structures of CuPc and CuPc- SO_3H are shown in Figure 1.

A semiempirical model based on the original Hamaker equation is then developed to calculate the Hamaker constant from the London dispersion coefficients and the densities of the particles. This model is used to predict values of the Hamaker constants of CuPc pigments.

In the present Article, the conventional notations A_{11} and A_{12} are used to denote Hamaker constants in vacuum for two like- and unlike-particles, while C_{11} and C_{12} are used to denote their London molecular dispersion coefficients. Two experimentally derived Hamaker constants A_{11} for CuPc particles have been reported in the literature.^{11,12} Among them, the value of $A_{11} = 0.2 \times 10^{-20} \text{ J}^{11}$ was estimated from certain mechanical strength properties by using some assumptions regarding (i) the detailed structure of a CuPc powder and the relationship of A_{11} to its mechanical properties and (ii) molecular distances of adjacent particles in the powder at close contact. This value is an order of magnitude lower than the values of ca. $(4\text{--}7) \times 10^{-20} \text{ J}$ calculated or measured for many organic materials. Because CuPc contains Cu and benzene rings, its density is higher than those of hydrocarbons, and hence the value of A_{11} for CuPc should be higher than $7 \times 10^{-20} \text{ J}$. For this reason, the accuracy of the above value of $0.2 \times 10^{-20} \text{ J}$ is questionable. A higher value of $A_{11} = 3.7 \times 10^{-20} \text{ J}$ for CuPc green (i.e., of chlorinated CuPc) was reported recently in ref 12, although it still appears to be too low for the similar reasons detailed above.

Hence, there is a need to obtain more accurate values of A_{11} (for CuPc), which would be useful for ink dispersion stability studies. In the present study, a TDDFT scheme is benchmarked for predictions of the dispersion coefficients of five molecules (H_2O , NH_3 , CO_2 , C_6H_6 , and pentane) and for predictions of the static dipole polarizabilities of three organometallic compounds (TiCl_4 , OsO_4 , and $\text{Ge}(\text{CH}_3)_4$). Next, this validated TDDFT scheme was used to determine the London dispersion coefficients (C_{11}) for the CuPc

molecule. Because certain CuPc particles are stabilized by chemically attached sulfonate groups (SO_3H) at their surface, the C_{11} value for CuPc- SO_3H is also computed. The A_{11} values for two commonly available CuPc crystal polymorphs, α -CuPc and β -CuPc, are then calculated using the ideal crystal densities, as they are estimated from the crystal lattice parameters. In addition, the experimentally derived density of some commercial β -CuPc particles, stabilized by SO_3H , is used to obtain another estimate for A_{11} (β -CuPc). Our approach yields values of A_{11} that range from ca. 13 to $15 \times 10^{-20} \text{ J}$. While no reliable direct experimental data are available, the above predicted values are nonetheless thought to be more plausible and in turn more accurate than the previous estimates.

2. Theory and Computational Methods

2.1. London Dispersion Parameters and Hamaker Constants. In 1930, London¹³ performed a quantum mechanical analysis based on perturbation theory to predict the long-range dispersion interaction potential energy E_{dis} , between two atoms or molecules, 1 and 2, which is of the form:

$$E_{\text{dis}} = -\frac{C_{12}}{r^6} \quad (1)$$

where r is the separating distance between the atomic or molecular centers, and C_{12} is the dispersion coefficient as defined by London. Hamaker¹ integrated the interaction potential energies, based on the additivity concept as proposed by London, to calculate the total interaction energy between two macroscopic bodies (or particles, each consisting of either molecule 1 or 2):

$$E_{12} = - \int_{V_1} \int_{V_2} \frac{\rho_1 \rho_2 C_{12} \, dV_1 \, dV_2}{r^6} \quad (2)$$

where ρ_1 and ρ_2 are the number densities, and V_1 and V_2 are the volumes of particles 1 and 2, respectively. Given the above equation, the Hamaker constant is defined as

$$A_{12} \equiv \pi^2 C_{12} \rho_1 \rho_2 \quad (3)$$

The remaining terms in eq 2 produce a purely geometrical term upon integration.

The derivation that leads to the above relation is based on the following assumptions taken into consideration: (A) additivity: a pairwise summation of the individual contributions provides the total interaction; (B) continuous medium: integration over the volumes of the interacting bodies replaces the pairwise summation; (C) uniform material properties: each ρ and C_{11} are considered to be uniform over the total volume of the interacting bodies; and (D) medium: the above interaction is in a vacuum.

If the particles 1 are in a medium consisting of material 2, the following Hamaker constants are defined: in a vacuum, A_{11} , A_{22} , and A_{12} as above and for two particles, both of type 1, located in a medium 2 (particle 2), A_{121} . An approximate estimation of A_{121} has been proposed:⁹

$$A_{121} \approx A_{11} + A_{22} - 2A_{12} \quad (4)$$

and it is often assumed, based somewhat on London's theory and the assumption of $C_{12} \approx (C_{11}C_{22})^{1/2}$, that

$$A_{12} = \sqrt{A_{11}A_{22}} \quad (5)$$

It then follows that

$$A_{121} \approx (\sqrt{A_{11}} - \sqrt{A_{12}})^2 \quad (6)$$

The above results are also only applicable to nonretarded van der Waals interactions,¹⁴ which require that the interparticle distances are smaller than about 0.1 μm .¹⁵

In 1956, Lifshitz¹⁶ developed a macroscopic continuum theory for Hamaker constants based on quantum electrodynamics and quantum field theory. The Lifshitz theory requires data on the complex dielectric constants of each material at all frequencies. Because of a relativistic effect, the Hamaker constant is distance-dependent, or "retarded", beyond about 0.1 μm .^{15,17}

In the present study, only the nonretarded London dispersion coefficients are considered. An efficient computational model based on the time-dependent density functional theory (TDDFT) for C_{12} ^{18,19} has been chosen as described below. Moreover, a modified form of eq 3 was used to calculate the nonretarded Hamaker constants from C_{12} :

$$A_{12} = a\pi^2 C_{12} \rho_1 \rho_2 \quad (7)$$

where a is an empirical parameter, devised here to account for the shortcomings of assumptions A, B, and C mentioned above. In particular, assumption A ignores the many-body effects in the condensed phase. Assumption B ignores the intrinsic discontinuous nature of the materials, and assumption C does not take into account the possible nonuniform density variations of the macroscopic particles. In addition, the parameter a also accounts for the errors in the TDDFT calculations of dispersion coefficients (see section 4.4).

2.2. Time-Dependent DFT for Computing C_{12} . The nonretarded dispersion coefficient for molecules 1 and 2, averaged over all possible orientations, is given by the

Casimir–Polder relation:²⁰

$$C_{12} = \frac{3}{\pi} \int_0^\infty du \alpha^1(i\omega) \alpha^2(i\omega) \quad (8)$$

where $\alpha^X(i\omega)$ is the trace of the dipole polarizability tensor of molecule X ($=1$ or 2) evaluated at the imaginary frequency $i\omega$. The function $\alpha^X(i\omega)$ can be calculated by a TDDFT time propagation scheme as reported in ref 18 and implemented in the OCTOPUS code.²¹

To evaluate the Casimir–Polder integral for the dispersion coefficients in eq 8, the polarizabilities were calculated at the imaginary frequencies from the Gauss–Legendre integration schemes.

2.3. Benchmark Data. It is important to validate the accuracy of the TDDFT scheme described in section 2.2 for predictions of dispersion coefficients. The dispersion coefficients (C_{11}) of five molecules, H_2O , NH_3 , CO_2 , C_6H_6 , and pentane, have been used as a benchmark data. The reference values for these five molecules have been taken from the results of the dipole oscillator strength distribution (DOSD) method of Meath and co-workers.^{22–26}

Because CuPc is an organometallic compound, it is desirable to include some organometallic compounds in the benchmark set. However, we are unable to find any accurate dispersion coefficients for organometallic compounds from the literature. We have chosen to use the static dipole polarizabilities of three organometallic compounds, TiCl_4 , OsO_4 , and $\text{Ge}(\text{CH}_3)_4$, to benchmark the quality of the employed methods. The reference static dipole polarizability for OsO_4 is taken from a collision-induced light scattering experiment of Hohm and Maroulis,²⁷ and the reference value for TiCl_4 is from a combined experimental and theoretical study by the same authors.²⁸ The reference polarizability for $\text{Ge}(\text{CH}_3)_4$ is taken from a recent collision-induced light scattering experiment of Maroulis and Hohm.²⁹

We collected accurate Hamaker constants for six compounds (H_2O , pentane, decane, hexadecane, polystyrene, and poly(methyl methacrylate)) to obtain the parameter a in eq 7, and the reference Hamaker constants are taken from the accurate Lifshitz theory calculations by Hough and White.⁵

2.4. Computational Details. The molecular geometries of the selected chemical species were optimized with the M06-L density functional³⁰ and the 6-31+G(d,p) basis set.³¹ The OCTOPUS program has been employed for the TDDFT propagation calculations of the dispersion coefficients and polarizabilities as described in section 2.2.

OCTOPUS is a pseudopotential real space DFT program, in which electrons are described quantum-mechanically with DFT or TDDFT, nuclei are described classically as point particles, and interactions between electrons and nuclei are described with the pseudopotential approximation. We examined the convergence of the grid spacing with two pseudopotentials; one is the Hartwigsen–Goedecker–Hutter (HGH) type of pseudopotentials,³² which are relativistic separable dual-space Gaussian pseudopotentials. We also examined the FHI pseudopotentials developed by Fuchs and Scheffler³³ at Fritz-Haber-Institut.

We have tested the performance of 13 density functionals for the calculation of dispersion coefficients and static dipole

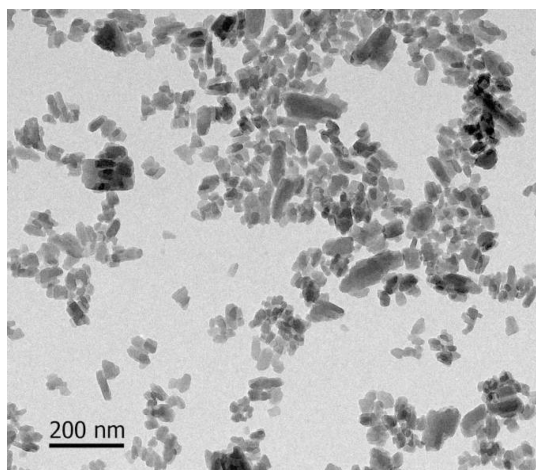


Figure 2. TEM image of β -CuPc pigment particles dried on a holey carbon TEM grid.

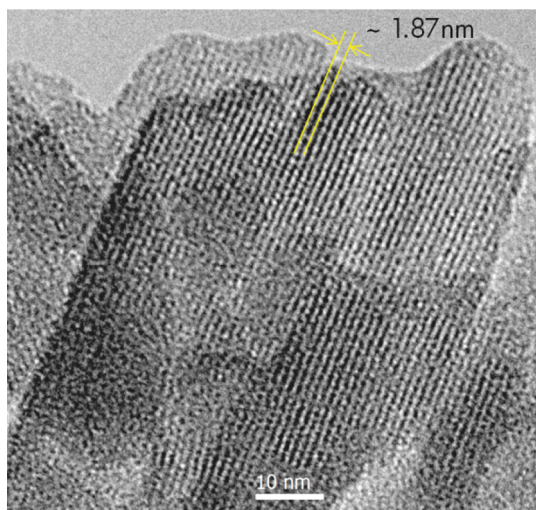


Figure 3. High-resolution TEM image of a β -CuPc pigment particle. Distinctive lattice fringes with a spacing of ~ 1.9 nm can be clearly observed.

polarizabilities. The tested density functionals include the SPZ local spin density approximation (LSDA),^{34–36} six generalized gradient approximations (GGAs), PW91,³⁷ PBE,³⁸ HCTH,³⁹ RPBE,⁴⁰ WC, and XLYP,⁴¹ and six hybrid GGAs (B3PW91,⁴² B3LYP,⁴³ B3P86,⁴³ PBE0,⁴⁴ O3LYP,^{45,46} and X3LYP⁴¹).

3. Experimental Characterization of the CuPc Pigment Particles

The CuPc particles were obtained from Cabot Corp. (MA) as a 10 wt % stable dispersion in water and were used as received. They consist of pure CuPc stabilized by chemically attached sulfonate groups. The particles were characterized with high-resolution (HR) TEM. As shown in Figure 2, their morphology is tubular-like or cubical-like. These particles are crystalline. Distinctive lattice fringes, extending up to the edges of the pigment particles, were observed, with a spacing of ~ 1.9 nm, which corresponds to the lattice constant of the β -CuPc structure (Figure 3). The thickness of the sulfonate groups is likely to be less than 0.5 nm on each

Table 1. Convergence of the Gauss–Legendre Quadrature Scheme for the Calculation of the Dispersion Coefficient (C_{11}) of Benzene^a

N^b	C_{11} (au)
4	1800.5
6	1796.0
8	1796.0
10	1796.0

^a TDDFT calculations with the SPZ local density functional, using the Hartwigsen–Goedecker–Hutter (HGH) pseudopotentials,³² and a grid spacing of 0.25 Å. ^b N denotes the number of imaginary frequencies ($i\omega$ in eq 8) for which the dynamic polarizabilities have been calculated, using the Gauss–Legendre integration scheme.

side. Hence, the particles are more than 99% β -CuPc and less than 1% CuPc-SO₃H.

Standard dynamic light scattering measurements performed with a Brookhaven ZetaPALS dynamic light scattering instrument at a wavelength of 659 nm, which has a BI-9000AT digital autocorrelator at a scattering angle of 90°, revealed an average hydrodynamic diameter of about 90 \pm 3 nm.

The ideal, or theoretical, particle densities for α - and β -CuPc were calculated on the basis of the crystal lattice parameters as follows:²⁶ (A) For α -CuPc, $a = 25.92$ Å, $b = 3.79$ Å, $c = 23.92$ Å, $\beta = 90^\circ$, $\rho_1 = 1.63$ g/cm³. (B) For β -CuPc, $a = 19.407$ Å, $b = 4.79$ Å, $c = 14.628$ Å, $\beta = 120^\circ$, $\rho_1 = 1.62$ g/cm³.

The density of the actual CuPc nanoparticles was also measured experimentally with the following method. A given mass m_T of a dispersion had a volume V_T at 25 °C and a dry weight m_p , as determined by drying in an oven at 50 °C for 3 days. Next, the particle density ρ_p was determined with the following equation and the measured values of m_T , m_p , and V_T :

$$V_T = \frac{m_p}{\rho_p} + \frac{m_T - m_p}{\rho_w} \quad (9)$$

where ρ_w is the literature density of water at 25 °C. The volumes of the particles and the water are assumed to be additive, because the particles are dispersed as a separate phase. The weight fraction of the particles was found to be 0.1005 ± 0.0004 , which compares well with the nominal value of 0.10. The particle density was found to be $\rho_p = 1.56 \pm 0.03$ g/cm³ (average of $n = 3$ measurements). This value is about 4% smaller than the ideal value above. The reasons for the small discrepancy are probably: (a) the presence of crystal imperfections or voids in the particles; (b) not accounting for the surface sulfonate groups and associated counterions; and (c) other experimental errors. A 4% discrepancy results in an 8% discrepancy in the value of A_{11} . Values of A_{11} for both values of the densities are reported.

4. Results and Discussion

4.1. Gauss–Legendre Integration for the Casimir–Polder Equation.

To determine a minimum number of data points while maintaining an accurate evaluation of the Casimir–Polder integral (eq 8), we benchmarked the Gauss–Legendre

Table 2. Convergence of Dispersion Coefficients and Dipole Polarizabilities with Grid Spacing^a

grid spacing (Å)		C ₁₁ (au)					static dipole polarizability α (au)		
		H ₂ O	NH ₃	CO ₂	C ₆ H ₆	C ₅ H ₁₀	TiCl ₄	OsO ₄	Ge(CH ₃) ₄
HGH ^b	0.20	50.4	93.4	162.1	1797	2000	99.0	50.9	87.6
	0.25	50.8	93.2	163.2	1796	2000	99.0	50.6	87.6
	0.30	52.6	92.3	167.0	1795	2000	99.1	50.1	87.6
	0.35	60.4	92.8	182.7	1796	1997	99.3	47.7	88.2
FHI ^c	0.20	50.1	92.6	161.8	1784	1978	97.8	50.6	87.2
	0.25	50.1	92.6	161.7	1781	1984	97.8	50.6	87.5
	0.30	49.7	92.3	161.4	1786	1987	98.2	50.6	87.3
	0.35	49.8	92.8	160.4	1785	1986	98.2	50.5	87.4

^a All calculations employed the SPZ LSDA density functional. ^b The Hartwigsen–Goedecker–Hutter (HGH) type of pseudopotentials.³²
^c The FHI pseudopotentials developed by Fuchs and Scheffler³³ at Fritz-Haber-Institut.

Table 3. Performance of Density Functionals for Dispersion Coefficients and Static Dipole Polarizabilities with the HGH Pseudopotentials

method	C ₁₁ (au)					static dipole polarizability α (au)				AMAPE ^c
	H ₂ O	NH ₃	CO ₂	C ₆ H ₆	C ₅ H ₁₀	MAPE ^a	TiCl ₄	OsO ₄	Ge(CH ₃) ₄	
best estimate ^d	45.3	89.0	158.7	1723	1905		101.4	51.0	83.2	
SPZ	50.8	93.2	163.2	1796	2000	5.8	99.0	50.6	87.6	2.8
XLYP	42.5	76.2	143.2	1547	1649	10.8	89.6	47.5	78.2	8.1
PW91	41.0	73.8	139.1	1512	1633	13.1	88.4	46.6	77.4	9.4
PBE	40.7	73.2	138.6	1505	1630	13.5	88.1	46.5	77.1	9.8
X3LYP	39.6	75.9	138.0	1523	1626	13.3	87.0	46.3	76.7	10.4
WC	40.2	72.4	137.5	1499	1633	14.1	88.1	46.1	76.9	10.1
B3LYP	41.3	74.9	137.0	1509	1606	13.3	86.6	46.1	76.0	10.9
RPBE	38.9	73.4	138.7	1502	1617	14.4	87.7	46.6	77.0	9.8
HCTH	40.5	73.4	135.4	1486	1607	14.4	87.0	46.2	76.8	10.4
PBE0	39.8	72.6	132.9	1475	1587	15.6	85.2	45.2	75.0	12.4
B3P86	37.6	72.1	132.5	1470	1578	16.9	85.3	45.2	74.6	12.6
O3LYP	39.1	70.9	130.7	1445	1542	17.4	84.8	45.2	74.4	12.8
B3PW91	37.1	71.0	131.9	1458	1564	17.7	84.9	45.1	74.3	12.9
										15.3

^a MAPE is the mean absolute percentage error for the dispersion coefficients, which is calculated as

$$\text{MAPE} = \sum_{i=1}^5 \frac{|C_{11}^{\text{cal},i} - C_{11}^{\text{best est.,}i}|}{C_{11}^{\text{best est.,}i}} \times 100\% / 5$$

^b MAPE is the mean absolute percentage error for the dipole polarizabilities, which is calculated as

$$\text{MAPE} = \sum_{i=1}^3 \frac{|\alpha_i^{\text{cal}} - \alpha_i^{\text{best est.}}|}{\alpha_i^{\text{best est.}}} \times 100\% / 3$$

^c AMAPE is the average of the two MAPE. ^d The best estimates of the dispersion coefficients (C_{11}) are taken from the DSOD results of Meath and co-workers.^{22–26} The reference static dipole polarizability for OsO₄ is taken from a collision-induced light scattering experimental study by Hohm and Maroullis,²⁷ and the reference value for TiCl₄ is from a combined experimental and theoretical study by the same authors.²⁸ The reference polarizability for Ge(CH₃)₄ is taken from a recent collision-induced light scattering experiment of Maroullis and Hohm.²⁹

integration scheme against the calculation of the dispersion coefficient of benzene. As shown in Table 1, a four-digit accuracy of the dispersion coefficient was found with the use of the six-point Gauss–Legendre quadrature scheme. We therefore used the six-point Gauss–Legendre integration in all of our calculations.

4.2. Convergence for Grid Spacing. The OCTOPUS code²¹ performs a TDDFT calculation on a real space mesh. Therefore, it is important to examine the convergence of dispersion coefficients and polarizabilities with the grid spacing. Table 2 gives the results for different grid spacings with the SPZ functional^{35,36} and two pseudopotentials (HGH³² and FHI³³). As shown in Table 2, with the grid spacing of 0.25 Å, the dispersion coefficients and static dipole polarizabilities are converged to better than 1% for both

pseudopotentials. Therefore, the grid spacing of 0.25 Å is used to test the performance of different density functionals.

4.3. Benchmarking Density Functionals for Dispersion Coefficients and Static Dipole Polarizabilities. The performance of 13 density functionals for predictions of dispersion coefficients and static dipole polarizabilities is presented in Table 3 (with the HGH pseudopotentials³²) and Table 4 (with the FHI pseudopotentials³³). Two statistical errors are tabulated in both tables; mean absolute percentage error (MAPE) is a measure of accuracy of different functionals, whereas AMAPE is an average of the MAPEs for dispersion coefficients and for static dipole polarizabilities.

As shown in Tables 3 and 4, the SPZ functional gives the best performance for dispersion coefficients and static polarizabilities for both HGH and FHI pseudopotentials.

Table 4. Performance of Density Functionals for Dispersion Coefficients and Static Dipole Polarizabilities with the FHI Pseudopotentials

method	C_{11} (au)					static dipole polarizability α (au)					
	H ₂ O	NH ₃	CO ₂	C ₆ H ₆	C ₅ H ₁₀	MAPE ^a	TiCl ₄	OsO ₄	Ge(CH ₃) ₄	MAPE ^b	AMAPE ^c
best estimate ^d	45.3	89.0	158.7	1723	1905		101.4	51.0	83.2		
SPZ	50.1	93.2	163.2	1796	2000	5.5	98.1	50.6	87.5	3.0	4.3
XLYP	41.6	76.2	143.2	1547	1649	11.2	88.8	47.3	77.8	8.7	9.9
PW91	40.2	73.8	139.1	1512	1633	13.4	87.7	46.5	77.1	9.9	11.7
PBE	40.0	73.2	138.6	1505	1630	13.8	87.4	46.4	76.7	10.2	12.0
RPBE	40.2	73.4	138.7	1502	1617	13.8	87.1	46.5	76.6	10.3	12.1
X3LYP	38.9	75.9	138.0	1523	1626	13.6	86.2	46.1	76.4	10.9	12.3
WC	39.6	72.4	137.5	1499	1633	14.4	87.3	46.1	76.7	10.5	12.4
HCTH	39.4	73.4	135.4	1486	1607	14.9	86.4	46.1	76.3	10.9	12.9
B3LYP	38.5	74.9	137.0	1509	1606	14.5	85.8	45.9	75.7	11.4	13.0
PBE0	36.9	72.6	132.9	1475	1587	16.9	84.4	45.1	74.8	12.8	14.8
B3P86	36.8	72.1	132.5	1470	1578	17.2	84.5	45.0	74.3	13.0	15.1
B3PW91	36.6	71.0	131.9	1458	1564	17.9	84.1	44.9	74.0	13.3	15.6
O3LYP	36.9	70.9	130.7	1445	1542	18.4	84.1	45.1	74.1	13.2	15.8

^a MAPE is the mean absolute percentage error for the dispersion coefficients, which is calculated as

$$\text{MAPE} = \sum_{i=1}^5 \frac{|C_{11}^{\text{cal},i} - C_{11}^{\text{best est.,}i}|}{C_{11}^{\text{best est.,}i}} \times 100\%/5$$

^b MAPE is the mean absolute percentage error for the dipole polarizabilities, which is calculated as

$$\text{MAPE} = \sum_{i=1}^3 \frac{|\alpha_i^{\text{cal}} - \alpha_i^{\text{best est.}}|}{\alpha_i^{\text{best est.}}} \times 100\%/3$$

^c AMAPE is the average of the two MAPE. ^d The best estimates of the dispersion coefficients (C_{11}) are taken from the DSOD results of Meath and co-workers.^{22–26} The reference static dipole polarizability for OsO₄ is taken from a collision-induced light scattering experimental study by Hohm and Maroullis,²⁷ and the reference value for TiCl₄ is from a combined experimental and theoretical study by the same authors.²⁸ The reference polarizability for Ge(CH₃)₄ is taken from a recent collision-induced light scattering experiment of Maroullis and Hohm.²⁹

Table 5. Comparison of Predicted A_{11} ($\times 10^{-20}$ J) Values to the “Best Estimates” of Hough and White

material	C_{11} (au) ^a	ρ_1 (g/cm ³)	A_{11} best estimate ^b	A_{11}	A_{11}	A_{11}
				$a = 1.0$	$a = 0.6883$	$a = 0.6815$
H ₂ O	50.8	1.000	3.70	5.38	3.70	3.66
pentane	2000	0.626	3.75	5.16	3.55	3.52
decane	7649	0.730	4.72	6.89	4.74	4.70
hexadecane	19 368	0.770	5.23	7.67	5.28	5.23
polystyrene	3599	1.050	6.58	10.11	6.95	6.89
PMMA	2324	1.190	7.11	11.32	7.79	7.71
MAPE ^c				48.08	3.66	3.48

^a All dispersion coefficients are calculated with the SPZ functional and the HGH pseudopotentials using a grid spacing of 0.25 Å. ^b Taken from Hough and White.⁵ ^c MAPE is the mean absolute percentage error for Hamaker constants, which is calculated as

$$\text{MAPE} = \sum_{i=1}^6 \frac{|A_{11}^{\text{cal},i} - A_{11}^{\text{best est.,}i}|}{A_{11}^{\text{best est.,}i}} \times 100\%/6$$

However, with the FHI pseudopotentials, we encountered some self-consistent field convergence problems for CuPc, so we have chosen to use the SPZ functional and the HGH pseudopotentials with a grid spacing of 0.25 Å for the calculation of Hamaker constants.

4.4. Estimation of the Parameter a in Eq 7. We employed eq 7 to compute Hamaker constants. Because the TDDFT calculated C_{11} values are used in eq 7 to compute the Hamaker constant, the parameter a explicitly corrects the error in the TDDFT calculation as well as the deficiencies of the three assumptions mentioned in section 2.1. One way to determine the parameter a is to use the accurate Hamaker constant of water determined by Hough and White as the

“standard”. Using the value of $A_{11} = 3.7 \times 10^{-20}$ J and the calculated C_{11} for H₂O, it is found that $a = 0.6883$. Another way of determining the parameter a is to minimize the MAPE for a benchmark set of Hamaker constants of H₂O, pentane, decane, hexadecane, polystyrene, and PMMA. The value for the optimized parameter a is found to be 0.6815 by this minimization. It is encouraging that this optimized parameter differs insignificantly from the value of 0.6883 determined by using the Hamaker constant of H₂O.

Table 5 lists the Hamaker constants calculated by using $a = 1.0$ (the same as the original Hamaker eq 3), $a = 0.6883$ (determined from the A_{11} of H₂O), and $a = 0.6815$ (optimized against the benchmark set of six Hamaker constants). As

Table 6. Dynamic Dipole Polarizabilities $\alpha(i\omega)$ (au) and Dispersion Coefficients C_{11} (au)^a

molecule	$\alpha(i\omega)^b$						C_{11}
	$\omega = 0.01048$	$\omega = 0.06118$	$\omega = 0.18441$	$\omega = 0.48804$	$\omega = 1.47101$	$\omega = 8.58488$	
CuPc	598.31	528.15	373.25	201.66	54.49	2.40	78 926
CuPc-SO ₃ H	646.10	570.64	405.02	220.58	60.25	2.69	93 224

^a The dynamic polarizabilities and dispersion coefficients in this table are calculated with the SPZ functional and the HGH pseudopotentials using a grid spacing of 0.25 Å. ^b The values of ω are from the six-point Gauss-Legendre integration scheme.

Table 7. Calculated Values of A_{11} and A_{121} for CuPc Using $a = 0.6815$ in Eq 7

particle	ρ_1 (g/cm ³)	$A_{11} \times 10^{-20}$ (J) ^a	$A_{121} \times 10^{-20}$ (J)	comment
α -CuPc	1.63	14.73	3.66	ideal density
β -CuPc	1.62	14.66	3.63	ideal density
β -CuPc	1.56	13.52	3.07	measured density

^a The Hamaker constants are calculated with the C_{11} of CuPc in Table 6.

shown in Table 5, the original Hamaker equation ($a = 1$) gives large errors as compared to the Lifshitz theory. The MAPE for $a = 1.0$ is about 50%, which is 13 times larger than the MAPEs of $a = 0.6883$ or 0.6815 . Table 5 also shows that using $a = 0.6815$ is slightly more accurate than $a = 0.6883$, as shown by its smaller MAPE. Therefore, $a = 0.6815$ is used for the computation of Hamaker constants of the CuPc pigments.

4.5. Computation of Dispersion Coefficients and Hamaker Constants for CuPc. Using the SPZ functional and the HGH pseudopotentials, the dynamic dipole polarizabilities and dispersion coefficients for CuPc and CuPc-SO₃H have been calculated, and the results are shown in Table 6. The plots of the dynamic dipole polarizabilities are given in the Supporting Information.

For densities of α -CuPc and β -CuPc shown in section 3, the Hamaker constants for CuPc nanoparticles were determined in vacuum (A_{11}) and in water (A_{121}), and the results are listed in Table 7.

These A_{11} values are noticeably larger than the previously reported values of 0.2 and 3.7×10^{-20} J (see section 1). By being larger than A_{11} of polystyrene, the values computed here seem to be more reasonable, because the density of CuPc particles is much greater than that of polystyrene.

The effect of the surface sulfonate groups on the total value of A_{11} is expected to be small. Using the values of C_{11} for CuPc and CuPc-SO₃H the estimated volume fraction of CuPcSO₃H should alter the computed value of A_{11} by no more than 1–2%. Such a correction may be more important for much smaller CuPc nanoparticles ($d < 10$ nm), but less important for larger nanoparticles ($d > 200$ nm). Because the relative uncertainties in the particle density, the C_{11} computation, and the used value of a are larger than 2%, the effect of the SO₃H groups on A_{11} of the 90 nm β -CuPc particles will be ignored.

The predicted values of A_{121} are also listed in Table 7. The relative uncertainty of A_{121} is larger than that of A_{11} . These values look to be plausible estimates of the Hamaker constants, which can be used as input into the DLVO theory^{47,48} for estimating colloidal stability. Having these values for A_{11} ((13–15) $\times 10^{-20}$ J), rather than the 0.2 and

3.7×10^{-20} values, makes a big difference in the computation of A_{121} . If the value of $A_{11} = 3.7 \times 10^{-20}$ J were used, the resulting A_{121} value would be predicted to be zero, and this would have a big impact on the predictions of the DLVO theory.

4.6. Limitations of the Proposed Model. As shown in the previous sections, a semiempirical parameter a is used to connect the Hamaker theory to the more accurate Lifshitz theory. The advantage of this model is that the experimental inputs for eq 7 are the densities of the particles, which are much easier to obtain than the experimental inputs for the Lifshitz theory, that requires detailed molecular and macroscopic information on the dielectric and/or optical properties of the material over a wide frequency range.⁵ However, one limitation of the model proposed in the present study is that the training set of the parameter a includes only the Hamaker constants of water, hydrocarbons, and polymers (PMMA and polystyrene). The transferability of the parameter a may be a concern for other type of materials. We expect that the accuracy of our model may be degraded for ionic crystals or metal clusters due to the presence of a large amount of complicated electrostatic and screening many-body interactions in these materials. Another limitation is that our model needs a well-defined building block (for C_{11}) of the particle. This is not a problem for H₂O, hydrocarbons, crystals, or homopolymers, but a well-defined building block for a random copolymer or for a protein needs extra effort.

5. Conclusions

A TDDFT method has been benchmarked for the computation of the London dispersion coefficients and static dipole polarizabilities. The Hamaker constants for nonretarded van der Waals interactions were calculated from C_{11} , the densities of particles, and an empirical correction to the original Hamaker equation. The value of this empirical parameter a was determined to be 0.6815, by optimizing against a benchmark set of six accurate Hamaker constants. Using this procedure resulted in an MAPE of 3.5% for the predictions of A_{11} in the benchmark set.

After the methods for determining C_{11} and A_{11} were benchmarked, the dynamic dipole polarizabilities and C_{11} for two target molecules, CuPc and CuPc-SO₃H, were computed. The Hamaker constants for α -CuPc and β -CuPc particles, which are important in pigment dispersions, were predicted to be in the range from 13 to 15×10^{-20} J. Such values are much larger than the available literature values of 0.2×10^{-20} and 3.7×10^{-20} J, which were inferred indirectly from certain previously published experiments. Overall, the new A_{11} value for CuPc seems to be a reasonably rigorous and accurate estimate that is more in line with our

expectations of the values of the Hamaker constant for similar organically based compounds. It can be argued that the previously reported estimates of A_{11} for CuPc are too low. While the current results suggest that the present method yields reliable predictions, more extensive tests are needed. In such tests, additional estimates of C_{11} and A_{11} may be calculated and compared to other reliable literature data or predictions.

Acknowledgment. This work was supported by HP Laboratories, Hewlett-Packard Co. We thank the developers of the OCTOPUS code for making this excellent computer program freely available to the scientific community. We are grateful to Mr. Eric Wu for providing computational resources for this work.

Supporting Information Available: Cartesian coordinates and the plots of the dynamic polarizabilities of CuPc molecules. This material is available free of charge via the Internet at <http://pubs.acs.org>.

References

- (1) Hamaker, H. C. *Physica* **1937**, *4*, 1058.
- (2) Das, S.; Sreeram, P. A.; Raychaudhuri, A. K. *Nanotechnology* **2007**, *18*, 35501.
- (3) Farmakis, L.; Lioris, N.; Kohadima, A.; Karaiskakis, G. *J. Chromatogr., A* **2006**, *1137*, 231.
- (4) Dzyaloshinskii, I. E.; Lifshitz, E. M.; Pitaevskii, L. P. *Adv. Phys.* **1961**, *10*.
- (5) Hough, D. B.; White, L. R. *Adv. Colloid Interface Sci.* **1980**, *14*, 8.
- (6) Bowen, W. R.; Jenner, F. *Adv. Colloid Interface Sci.* **1995**, *56*, 201.
- (7) Ackler, H. D.; French, R. H.; Chiang, Y. M. *J. Colloid Interface Sci.* **1996**, *179*, 460.
- (8) Bergström, L. *Adv. Colloid Interface Sci.* **1997**, *70*, 125.
- (9) French, R. H. *J. Am. Ceram. Soc.* **2000**, *83*, 2117.
- (10) Kim, H.-Y.; Sofo, J. O.; Velez, D.; Cole, M. W.; Lucas, A. A. *Langmuir* **2007**, *23*, 1735.
- (11) Li, Q.; Feke, D. L.; Manas-Zloczower, I. *Powder Technol.* **1997**, *92*, 17.
- (12) Hui, D.; Nawaz, M.; Morris, D. P.; Edwards, M. R.; Saunders, B. R. *J. Colloid Interface Sci.* **2008**, *324*, 110.
- (13) London, F. Z. *Physik* **1930**, *60*, 245.
- (14) Kaplan, I. G. *Intermolecular Interactions*; Wiley: Hoboken, NJ, 2006; p 72.
- (15) Calbi, M. M.; Gatica, S. M.; Velez, D.; Cole, M. W. *Phys. Rev. A* **2003**, *67*, 33201.
- (16) Lifshitz, E. M. *Sov. Phys.* **1956**, *2*, 73.
- (17) Parsegian, V. A. In *Physical Chemistry: Enriching Topics from Colloid and Surface Science*; Olphen, H. V., Mysels, K. J., Eds.; Theorex: La Jolla, CA, 1975; p 27.
- (18) Marques, M. A. L.; Castro, A.; Mallochi, G.; Mulas, G.; Botti, S. *J. Chem. Phys.* **2007**, *127*, 14107.
- (19) Botti, S.; Castro, A.; Andrade, X.; Rubio, A.; Marques, M. A. L. *Phys. Rev. B* **2008**, *78*, 35333.
- (20) Casimir, H. B. G.; Polder, D. *Phys. Rev.* **1948**, *73*, 360.
- (21) Castro, A.; Marques, M. A. L.; Appel, H.; Oliveira, M.; Rozzi, C.; Andrade, X.; Lorenzen, F.; Gross, E. K. U.; Rubio, A. *Phys. Status Solidi B* **2006**, *243*, 2465.
- (22) Margoliash, D. J.; Meath, W. J. *J. Chem. Phys.* **1978**, *68*, 1426.
- (23) Jhanwar, B. L.; Meath, W. J. *Chem. Phys.* **1982**, *67*, 185.
- (24) Jhanwar, B. L.; Meath, W. J. *Mol. Phys.* **1980**, *41*, 1061.
- (25) Kumar, A.; Meath, W. J. *Mol. Phys.* **1992**, *75*, 311.
- (26) Wu, Q.; Yang, W. *J. Chem. Phys.* **2002**, *116*, 515.
- (27) Hohm, U.; Maroulis, G. *J. Chem. Phys.* **2004**, *121*, 104118.
- (28) Hohm, U.; Maroulis, G. *J. Chem. Phys.* **2006**, *124*, 124312.
- (29) Hohm, U.; Maroulis, G. *Phys. Rev. B* **2007**, *76*, 32504.
- (30) Zhao, Y.; Truhlar, D. G. *J. Chem. Phys.* **2006**, *125*, 194101.
- (31) Hehre, W. J.; Radom, L.; Schleyer, P. v. R.; Pople, J. A. *Ab Initio Molecular Orbital Theory*; Wiley: New York, 1986; p 125.
- (32) Hartwigsen, C.; Goedecker, S.; Hutter, J. *Phys. Rev. B* **1998**, *58*, 3641.
- (33) Fuchs, M.; Scheffler, M. *Comput. Phys. Commun.* **1999**, *119*, 67.
- (34) Kohn, W.; Sham, L. J. *Phys. Rev.* **1965**, *140*, 1133.
- (35) Slater, J. C. *Quantum Theory of Molecular and Solids. Vol. 4: The Self-Consistent Field for Molecular and Solids*; McGraw-Hill: New York, 1974; p 136.
- (36) Perdew, J. P.; Zunger, A. *Phys. Rev. B* **1981**, *23*, 5048.
- (37) Perdew, J. P. In *Electronic Structure of Solids '91*; Ziesche, P., Eschig, H., Eds.; Akademie Verlag: Berlin, 1991; p 11.
- (38) Perdew, J. P.; Burke, K.; Ernzerhof, M. *Phys. Rev. Lett.* **1996**, *77*, 3865.
- (39) Hamprecht, F. A.; Cohen, A. J.; Tozer, D. J.; Handy, N. C. *J. Chem. Phys.* **1998**, *109*, 6264.
- (40) Hammer, B.; Hansen, L. B.; Norskov, J. K. *Phys. Rev. B* **1999**, *59*, 7413.
- (41) Xu, X.; Goddard, W. A. *Proc. Natl. Acad. Sci. U.S.A.* **2004**, *101*, 2673.
- (42) Becke, A. D. *J. Chem. Phys.* **1993**, *98*, 5648.
- (43) Stephens, P. J.; Devlin, F. J.; Chabalowski, C. F.; Frisch, M. J. *J. Phys. Chem.* **1994**, *98*, 11623.
- (44) Adamo, C.; Barone, V. *J. Chem. Phys.* **1999**, *110*, 6158.
- (45) Hoe, W.-M.; Cohen, A. J.; Handy, N. C. *Chem. Phys. Lett.* **2001**, *341*, 319.
- (46) Handy, N. C.; Cohen, A. J. *Mol. Phys.* **2001**, *99*, 403.
- (47) Derjaguin, B.; Landau, L. *Acta Physico Chemica URSS* **1941**, *14*, 633.
- (48) Verwey, E. J. W.; Overbeek, J. T. G. *Theory of the Stability of Lyophobic Colloids*; Elsevier: Amsterdam, 1948; p 100.